Materials Science and Technology (MS&T) 2012
October 7-11, 2012, Pittsburgh, Pennsylvania

Titanium Alloys for Demanding Applications

NUMERICAL AND EXPERIMENTAL INVESTIGATION OF LASER ASSISTED SIDE MILLING OF Ti6Al4V ALLOY

Hassan Zamani [1], Jan-Patrick Hermani [2], Bernhard Sonderegger [1], Christof Sommitsch [1]

[1] Institute for Materials Science and Welding, Graz University of Technology, Kopernikusgasse 24/I, Graz 8010, Austria
[2] Frauenhofer Institute for Production Technology IPT, Steinbachstrasse 17, 52074 Aachen, Germany

Keywords: Laser assisted machining, Ti-6Al-4V, Side milling, FEM, Cutting forces

Abstract

When milling or cutting hard materials, extensive tool wear is a common problem. One strategy for increasing the lifetime of tools is to preheat the material instantaneously by external heat sources, e.g. a laser beam before processing. This study focusses on the simulation of laser assisted side milling with the laser beam located on the cutting edge and moving synchronously with the cutter. This approach increases the heat input efficiency and lowers the cutting force and tool wear. A three dimensional finite element model in DEFORM 3D was set up to predict the cutting forces in the milling process with and without an additional laser heat source. Two different material constitutive models (Johnson-Cook and Calamaz modified J-C material model) were applied in the simulation of a Ti-6Al-4V alloy workpiece. A good agreement of the J-C material model with experimental findings is achieved.

Introduction

Today, more than 50% of raw titanium is used for production of Ti-6Al-4V. This fact indicates the importance of this alloy in various industries from aerospace to medical engineering. The reason relates to the unique profile of this alloy, which comprises high strength (even at temperatures up to 400°C), high strength to weight ratio and excellent corrosion resistance. Restricting the applications is the processing; the machining of Titanium is costly due to the high tool wear and the productivity is low due to limited cutting speed [1]. To overcome these difficulties, heating the material is a solution and consequently, heat input management is necessary. Still, heating can lead to side effects such as hot crack susceptibility, microstructure transformation and oxidation in the machined part. Locally heating the material in front of cutting zone using a laser beam, called laser-assisted-machining, has been investigated for 30 years [2], causing softening effects and subsequently a reduction of tool wear. Nevertheless, no modular and scalable tool system with integrated laser as one piece of equipment is available. The Fraunhofer IPT has developed and successfully realized a new concept of laser-assisted milling with spindle and tool integrated laser beam guiding. [3].The difference between the novel system and common laser-assisted milling can be found, first, in the position of the laser spot. In contrast to the conventional systems, the laser beam is placed directly on the cutting surface by an integrated mirror within the rotating machine spindle. Along with the practical efforts, a thermo-mechanical process model for the laser assisted machining of high strength metallic and

ceramic materials reduces time consuming testing periods. A finite element model (FEM) for the corresponding process was set up to predict required process parameters for different materials, operation modes and components geometries.

Experimental Setup

The experiments were performed on a Satisloh GI 3+2 axis machining center with Bosch Rexroth MTX P60 NC control and with optical and mechanical interfaces which are integrated into spindle and tool (see Figure 1). The process gas is supplied over a rotary lead through interface on the spindle housing for cooling optical and mechanical components. Furthermore, the process gas prevents chips from entering the beam path, which protects the optical components and supports the thermal process efficiency. An IPG YLS high power fiber laser (wavelength: 1070 mm) with a maximum power of 6 KW, was applied for providing the laser radiation. The diverging laser beam is collimated by an aspheric lens and propagates through the hollow shaft of the spindle. A tool integrated focusing lens forms a converging laser beam which is projected by two high reflection mirrors onto the workpiece directly in front of the cutting insert. In order to prevent the irradiation of already machined surface, the laser power is switched on/off at entrance and exit points, respectively. The laser power is modified according to the chip thickness during one revolution in the milling process. All experiments were conducted with round inserts (RDHX 07 02 M0T FLP) at a fixed depth of cut of 0.5 mm using TiAlN-coated cemented carbide cutting material. The maximum laser power varied from 0 to 1428 W, while the laser spot diameter was 1 mm. The fixed distance between the insert and the center of the laser spot (arc length) was 5 mm. Furthermore, the trials were conducted at different cutting velocities and feed rates with a tool diameter of 24 mm and a cutting width of 8 mm. The workpiece material was forged Ti-6Al-4V in annealed, and stress relieved condition. During the machining experiments a piezo-based three dimensional force measurement determined the process forces in 3 directions. For one path the maximum forces in each revolution (with a measurement frequency of 200 to 450 Hz) were averaged. Flank wear analysis was conducted with an optical microscope.

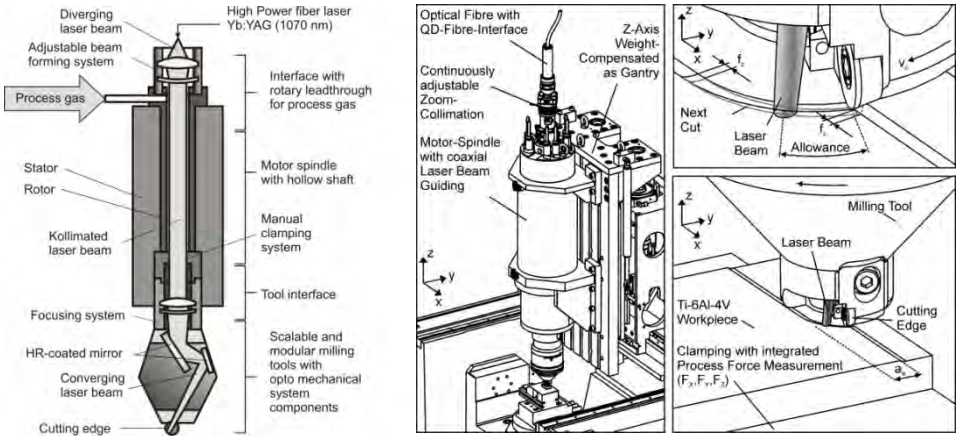

Figure 1. The working principle of the novel laser-assisted-milling [3].

Experimental Results

Effect of Cutting Velocity on Force Reduction

Figure 2 illustrates the effect of cutting velocity on the cutting forces for feed rates 70 and 90 µm/rev with laser (laser power: 1250 W) and without laser. With increasing cutting velocity, the

heat generation due to friction at the interface area increases, leading to the velocity-caused softening of the workpiece and consequently a reduction in the main cutting force (F_Y). This effect is more remarkable as the cutting velocity exceeds 150 m/min. In order to keep the accuracy of the force measurement, the tests were performed with cutting velocities up to 100 m/min. However, in the laser assisted milling, increasing the cutting velocity decreases the time for the heat transfer; hence, the cutting force reduction decreases, but the cutting forces are less than the milling without laser.

Effect of Laser Power on Force Reduction

Figure 3 presents the effect of laser power on the cutting forces at two different milling speeds (25 and 50 m/min). Generally, with increasing laser power, the forces are reduced. However, the reduction of forces is more pronounced in the Z and Y direction. Furthermore, the experimental results show the reduction of main cutting force (F_Y) more regularly than the force in direction normal to the milling surface (F_Z). The reason of the dissimilarity in reduction of forces in Z direction can be found in the chip sticking on the tool tip at low feed rates. As it can be seen in Figure 3, the reduction of F_Z goes into regularly with increasing the feed rate and also cutting velocity. The influence of laser power on the forces in the feed direction is not significant. These forces (F_X) are more sensitive to the feed rate.

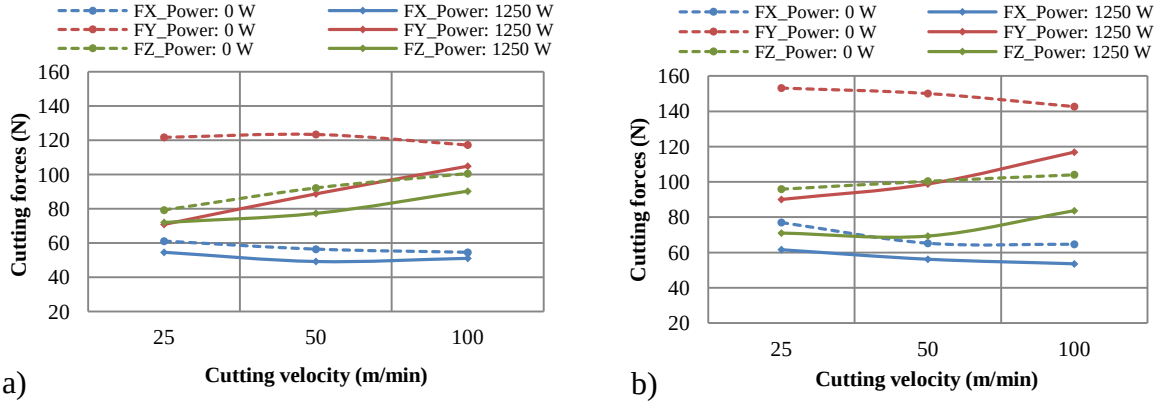

Figure 2. The effect of cutting velocity on cutting forces (a) feed rate 70 and (b) 90 µm/rev.

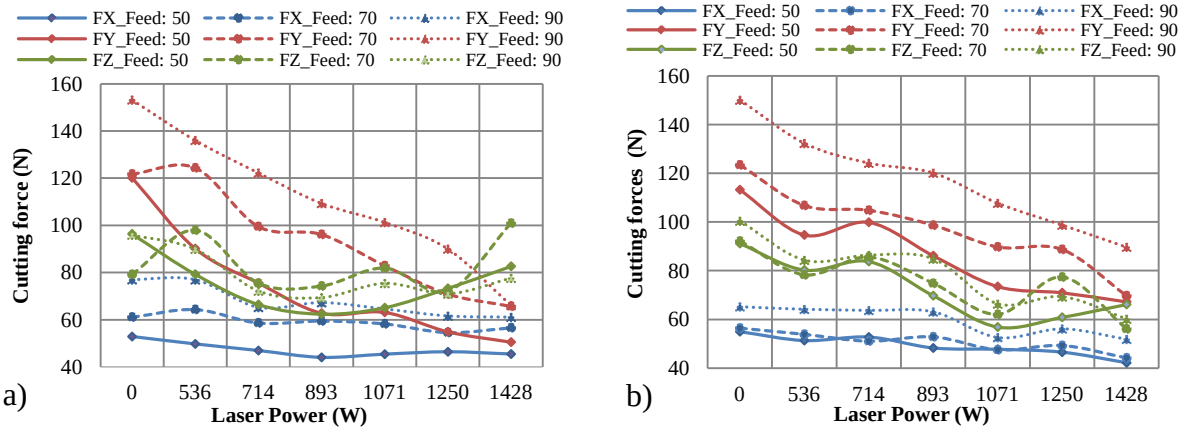

Figure 3. The effect of laser power on cutting forces (a) cutting velocity 25 and (b) 50 m/min.

Effects of Tool Wear on Force Reduction

Figures 4 and 5 show the forces' dependence on the material removal volume for the side milling process with/without laser heating (cutting velocity: 57 m/min, feed rate: 80 µm/rev, laser power: 900 W). It can be seen that the forces increase with time in both processes, but the increase is slower in the case of laser assisted milling. The reason is the slow change of tool tip geometry from sharp into round, which changes the stress state and contact area.

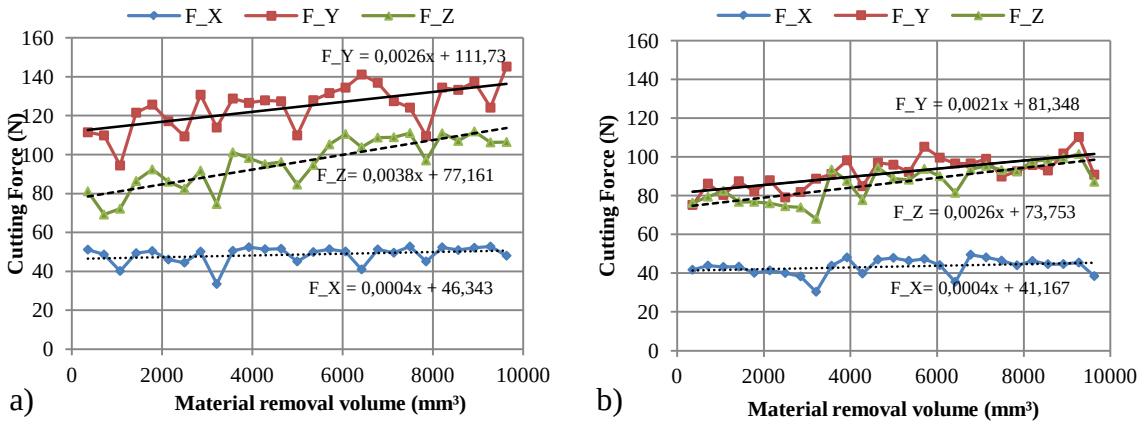

Figure 4.(a)The effect of milling time on the processes forces without laser and (b) with laser.

3-D FEM Simulation of Laser-assisted Machining

The commercial software DEFORM 3D has been used to set up a thermo-mechanical FEM model for the laser-assisted machining process. The implicit Lagrange mesh formulation provides can handle large deformations, but requires the frequent remeshing. The software supports automatic local remeshing, based on the impacted weighting factors. In the regions with high strain, strain rate and temperature, the generated mesh is finer (in the primary shear zone and the area near the tool tip) [4]. The model consists of the workpiece as a rigid-plastic part and the tool as a rigid body with tetrahedral elements for both. The thermal boundary conditions (convection and radiation) were considered by applying the convection heat transfer coefficients and the emissivity to the all elements with external contact. Tool movement was defined as rotation around the vertical axes and a constant velocity in the feed direction, while the coordinate system (mill center) moves according to the tool. The bottom surface of the workpiece was fixed in three directions. Based on the Zorev's model [5], the tool-chip contact area is divided into two regions according to the stress state on the rake face; sticking, governed by high normal stress, and otherwise sliding. Therefore, the tangential shear stresses on the tool surface cannot exceed the yield shear stress of chip material. The following relations express the frictional condition at the tool-chip interface:

$$\begin{aligned} \tau &= \mu\sigma_n, && \text{if} && \mu\sigma_n < \bar{m}\frac{\sigma_{eq}}{\sqrt{3}} \\ \tau &= \bar{m}\frac{\sigma_{eq}}{\sqrt{3}}, && \text{if} && \mu\sigma_n \geq \bar{m}\frac{\sigma_{eq}}{\sqrt{3}} \end{aligned} \qquad (1)$$

where σ_n is normal stress, τ is shear stress, $\sigma_{eq}$is the equivalent flow stress, μ is Coulomb friction coefficient and $\bar{m}$ is shear factor. The value for $\bar{m}$ and μ were kept as a constant of 0.7 and 0.5,

respectively. The heat interface coefficient between tool and chip is taken as constant value 50 kW/m² K.

With the purpose of predicting the temperature field including the impact of the laser beam, a 3D moving laser heat source model (Figure 5) with respect to the boundary conditions and temperature depending thermo-physical material properties (form Mill [6]) was set up. The laser spot according to the absorbed laser power density reaches a maximum steady temperature as the laser moves along its diameter. In order to insert the laser power intensity as the input parameter, the local convection coefficient approaches to near zero. The model enables the ability to investigate the effect of laser power, laser spot size, and distance between insert and laser spot incident angle, rotation velocity and feed velocity on the resulting temperature field. Also, it is possible to vary the laser Power during one revolution of the mill according to the chip thickness. The 27 % absorbed energy portion in the process was estimated based on the formation of a melting surface during one rotation of the mill by several tests in different laser powers with a constant rotation velocity.

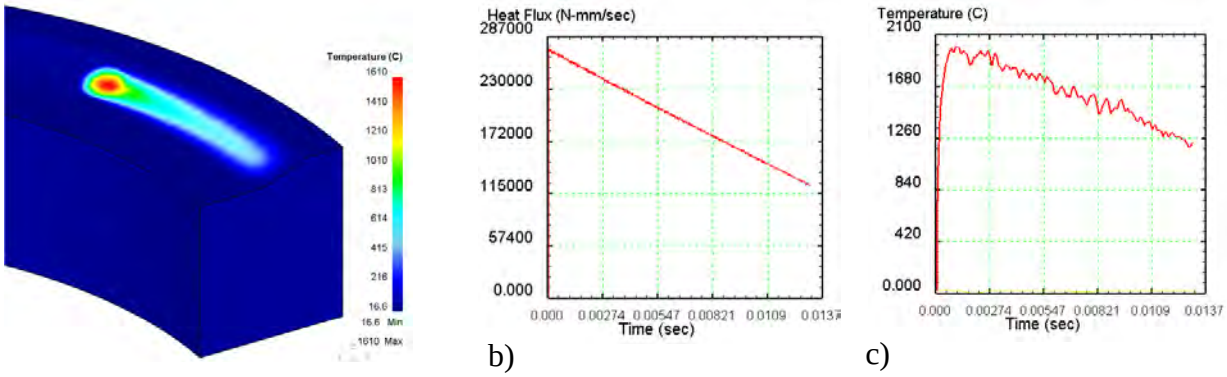

a) b) c)

Figure 5. 3D rotating laser heat source (Laser power with Gaussian distribution: 1000 W, angular velocity: 70 rad/s, feed velocity: 0.77 mm/s) (b) time dependent laser power (c) maximum temperature at the laser spot.

Material model

The empirical Johnson-Cook model [7] proposes the dynamic plastic flow especially for the large-scale analysis as a multiplicative function of strain, strain rate and temperature, where the first term is due to the strain hardening, second term expresses the strain rate sensitivity and last term is due to thermal softening:

$$\sigma_{eq} = (A + B\varepsilon^{n})\left(1 + C\ln\left(\frac{\dot{\varepsilon}}{\dot{\varepsilon}_0}\right)\right)\left(1 - \left(\frac{T - T_r}{T_m - T_r}\right)^{m}\right) \quad (2)$$

where σ_{eq} is the equivalent flow stress, ε is the equivalent plastic strain, $\dot{\varepsilon}$ is the equivalent plastic strain rate normalized with a reference strain rate $\dot{\varepsilon}_0$, T_m the melting temperature of material and T_r is the room temperature, while A, B, C, n and m are the material constants. Lee and Lin [8] determined these constants for strain values up to 0.35 mm/mm, strain rate up to 3300 s^{-1} and temperatures up to 1100°C.

Recently, a modified Johnson-Cook material model has been used by Calamaz and Sima [9,10]. The modifications consider the strain softening which is defined as decreasing the flow stress

with increasing strain over a critical strain value. This strain decreasing is justified by the dynamic recovery and/or recrystallization which lead to rearrangement of dislocations [11]. The modified model helps to predict better saw-tooth chip formation in titanium alloys. The reason can be explained with a hidden failure model (but here instead of update the value of stress components equal to zero, the stresses decreases continuously) in it with a critical stain value. The difference between the achieving chip morphology in 3D simulation can be seen in Figure 7a and b. It should be mentioned, the remarkable chip serration can be realized in 2D simulation with finer element size.

$$\sigma_{eq} = \left(A + B\varepsilon^{n}\left(\frac{1}{\exp(\varepsilon^{a})}\right)\right)\left(1 + C\ln\left(\frac{\dot{\varepsilon}}{\dot{\varepsilon}_0}\right)\right)\left(1 - \left(\frac{T - T_r}{T_m - T_r}\right)^{m}\right)\left(D + (1 - D)\left[\tanh\left(\frac{1}{(\varepsilon + p)^{r}}\right)\right]^{s}\right) \quad (3)$$

where $D = 1 - \left(\frac{T}{T_m}\right)^{d}$, $p = \left(\frac{T}{T_m}\right)^{b}$. In this model, parameter a sets the slope of flow stress decreasing after the critical strain value, b and p adjust the position and amount of maximum flow stress, d and D effects the magnitude of strain softening and minimum flow stress and parameter s controls the slope of the flow stress at high strains. The material constants for both models are listed in Table 1.

Table 1.Material constants

	A (MPa)	B (MPa)	C	m	n	T_m (°C)	a	b	r	d	s
JC-model [8]	724	683.2	0.035	1.0	0.47	1660	-	-	-	-	-
Mod. JC-model [10]	724	683.2	0.035	1.0	0.47	1660	2	5	2	1	0.05

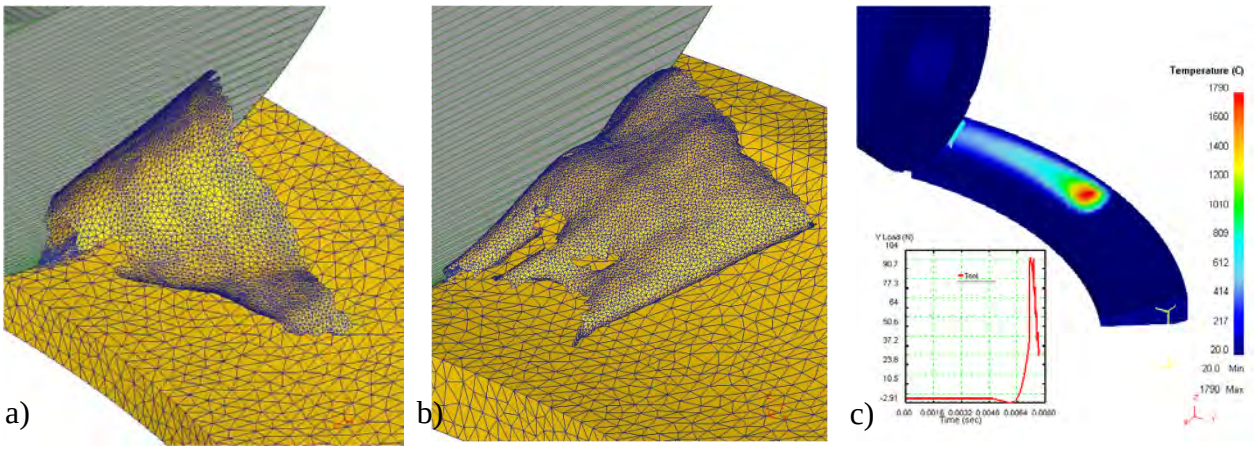

Figure 6. (a) Chip formation using JC-model (b) chip formation using modified JC-model (c) 3D FEM model of laser-assisted-side milling process.

Simulation Results and Model Validation

Analogous to the experimental trials, the maximum forces (corresponding to the maximum chip thickness) in 3D FEM simulation (Figure 6-c) were calculated. The simulation results were

compared with the experimental results in the different milling conditions with and without laser. The forces were calculated until an absolute maximum value and then the simulation went into the steady state for further temperature calculation. Figure 7 compares the cutting forces for both material models and experimental results. An excellent agreement for cutting forces in Y-direction was found for the J-C model. The modified model generally showed lower forces compared to J-C. The forces in Z-direction are about 10 % higher than the experimental results for J-C model. The force in X-direction presents higher reduction in laser assisted machining than the experimental results for J-C model, while modified J-C model does not change significantly with the laser power.

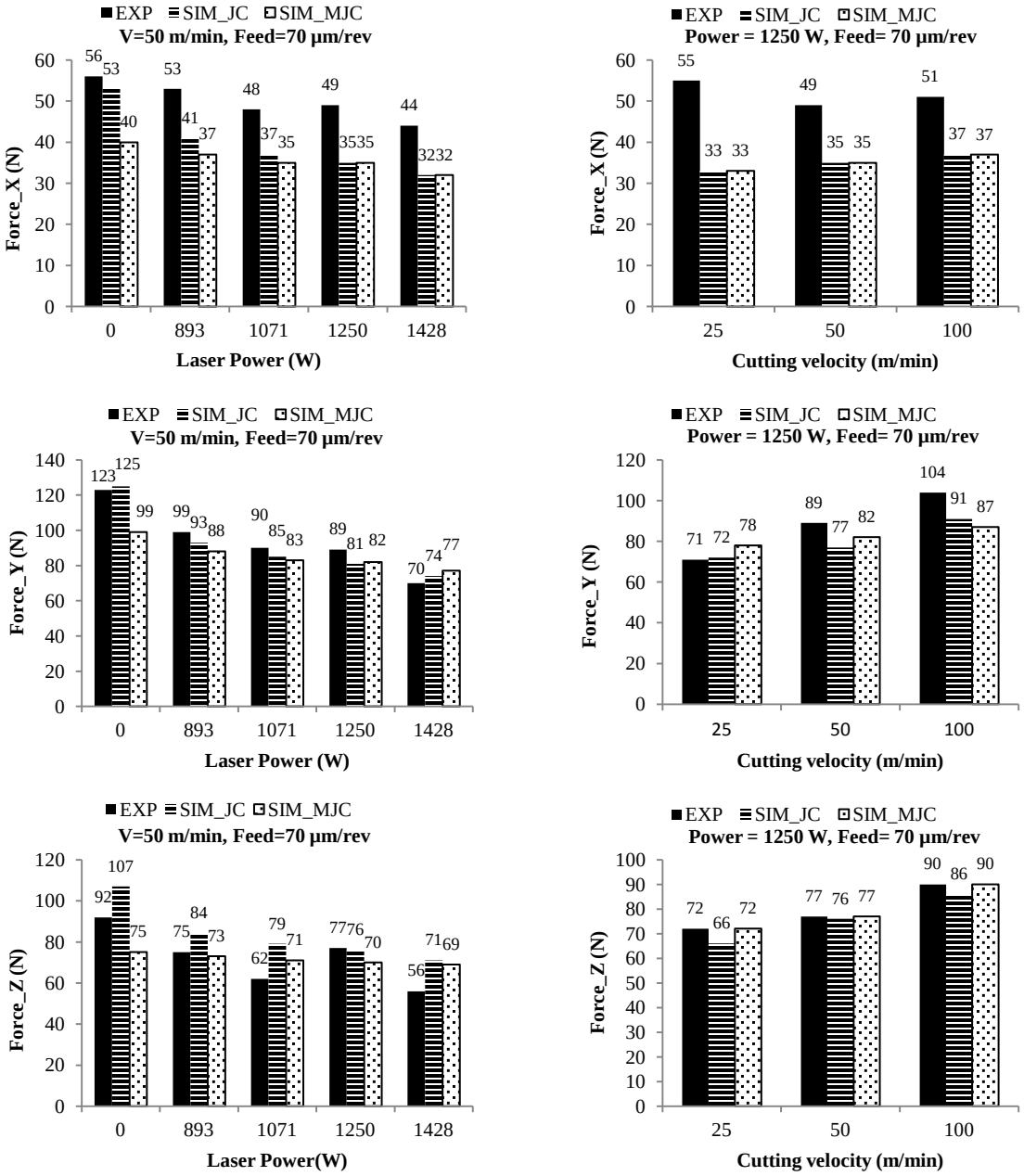

Figure 7. Comparison between simulation and experimental milling forces at the different milling conditions for JC-model (JC) and modified JC-model (MJC).

Conclusion

In this study, the results of laser-assisted milling of Ti-6Al-4V using TiAlN-coated cemented carbide cutting insert in different cutting conditions are presented. A significant reduction of forces was achieved with the optimization of the machining and laser parameters. The results showed a reduction of force in X-direction up to 25%, Y-direction up to 60% and Z-direction up to 65%. Furthermore, the tool wear value in the laser assisted milling expressed the higher tool life according to the material removal rate. Beside the experimental investigation, the effect of two material models (JC-model and modified JC-model) was studied. The results showed a good correlation between the experimental and simulated values for the forces in three directions with laser and without laser machining using the JC-model. The modified form stated generally lower level of forces which can be optimized by varying the related parameters based on the torsion test in high strain rates.

Acknowledgements

The research work presented in this paper is part of the TooLAM project, funded by European Union and the FFG within the EraSME program.

References

1. W. König, A. Zaboklicki, ‘‘Laserunterstützte Drehbearbeitung von Silizium-Nitrid-Keramik,” *VDI-Z 135*, 6 (1993), 34-39.
2. E. O. Ezugwu, Z. M. Wang, “Titanium alloys and their machinability—a review,” *Journal of Materials Processing Technology*, 68 (1997), 262–274.
3. C. Brecher, M. Emonts, C. J. Rosen and J. P. Hermani, ‘‘Laser-assisted Milling of Advanced Materials”*Physics Procedia*, 12 (2011), 599-606.
4. Deform-User Manual SFTC-Deform V10.0.2, Columbus (OH), USA, (2010).
5. N. Zorev, ‘‘Inter-relationship between shear processes occurring along tool face and shear plane in metal cutting,” *International Research in Production Engineering*, 1963, 42-49.
6. K. C. Mills, *Recommended Values of Thermo physical Properties for Selected Commercial Alloys*, Woodhead Publishing (2002), 217.
7. G.R. Johnson, W. H. Cook, ‘‘A constitutive model for metals subjected to large strains, high strain rates and high temperatures, ”*Proceedings of the Seventh International Symposium on Ballistics*, Hague, Netherlands, 54 (1983), 1-7.
8. W.S. Lee, C. F. Lin, “Plastic deformation and fracture behavior of Ti6Al4V alloy loaded with high strain rate under various temperatures,” *Materials Science and Engineering*, A241 (1998), 48–59.
9. M. Calamaz, D. Coupard, F. Girot, ‘‘A New Material Model for 2D Numerical Simulation of Serrated Chip Formation when Machining Titanium Alloy Ti–6Al–4V,” *International Journal of Machine Tools & Manufacture*,48 (2008), 275–288.
10. M. Sima, T. Özel, “Modified material constitutive models for serrated chip formation simulations and experimental validation in machining of titanium alloy Ti6Al4V,” *International Journal of Machine Tools and Manufacture*, 50 (2010), 943-960.
11. D. Ulutan, M. Sima, T.Özel, “Prediction of Ma chining Induced Surface Integrity using Elastic-Viscoplastic Simulations and Temperature-Dependent Flow Softening Material Models in Titanium and Nickel-based alloys,” *Advanced Material Research*, 223(2011), 401-410.